



Published in final edited form as:

J Am Chem Soc. 2020 January 22; 142(3): 1137–1141. doi:10.1021/jacs.9b07583.

Templated Collagen “Double Helices” Maintain Their Structure

I. Caglar Tanrikulu^{†,‡}, William M. Westler^{‡,§}, Aubrey J. Ellison[#], John L. Markley^{‡,§}, Ronald T. Raines^{*,†,‡,#}

[†]Department of Chemistry, Massachusetts Institute of Technology, Cambridge, Massachusetts 02139, United States

[‡]Department of Biochemistry, University of Wisconsin–Madison, Madison, Wisconsin 53706, United States

[#]Department of Chemistry, University of Wisconsin–Madison, Madison, Wisconsin 53706, United States

[§]NMRFAM, University of Wisconsin–Madison, Madison, Wisconsin 53706, United States

Abstract

The self-assembly of collagen-mimetic peptides (CMPs) that form sticky-ended triple helices has allowed the production of surprisingly stable artificial collagen fibers and hydrogels. Assembly through sticky ends requires the recognition of a single strand by a templated strand dimer. Although CMPs and their triple helices have been studied extensively, the structure of a strand dimer is unknown. Here, we evaluate the physical characteristics of such dimers, using disulfide-templated (PPG)₁₀ dimers as a model. Such “linked-dimers” retain their collagen-like structure even in the absence of a third strand, but only when their strands are capable of adopting a triple-helical fold. The intrinsic collagen-like structure of templated CMP pairs helps to explain the success of sticky-ended CMP association and changes the conception of new synthetic collagen designs.

Graphical Abstract

*Corresponding Author: rtraines@mit.edu.

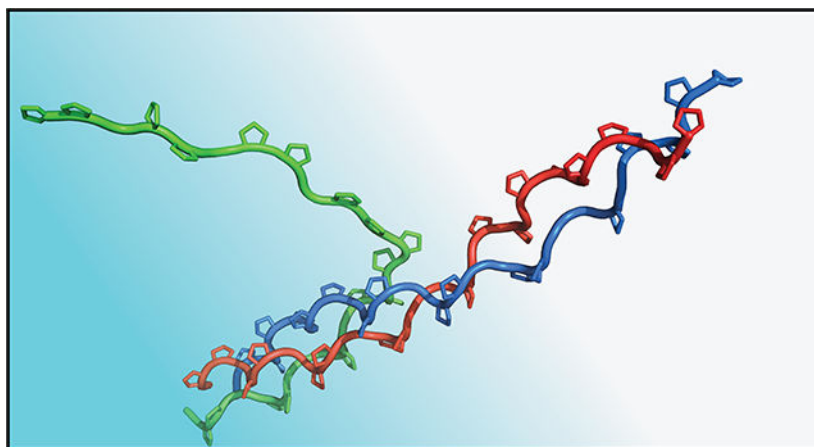
The authors declare no competing financial interest.

ASSOCIATED CONTENT

Supporting Information

The Supporting Information is available free of charge at <https://pubs.acs.org/doi/10.1021/jacs.9b07583>.

Procedures for peptide synthesis and purification; experimental and computational methods and additional data.



Collagen is the principal component of the extracellular matrix in vertebrates, constituting 70% of the dry weight of human skin.¹ The prominence of collagen—with functions ranging from resisting tension in one-to-three dimensions to setting a template for biomineralization and driving cellular differentiation—has made this protein a prime substrate for biomaterial applications.²

Collagens are characterized by Xaa-Yaa-Gly tripeptide repeats in their primary sequence, where the Xaa and Yaa residues are most often proline (Pro; P) and 4-hydroxyproline (Hyp; O), always followed by glycine (Gly; G).³ Such proline-rich sequences are predisposed to fold into left-handed polyproline type-II (PPII) helices, which can associate with other strands to form right-handed triple helices (Figure 1A). Assembly of natural collagen fibers is heavily regulated through chaperones, trimerization domains, and covalent crosslinks. The resulting triple helices can extend for ~1000 residues in fiber-forming collagens, prominent in skin, cartilage, and bone.³

Much of our molecular understanding of the collagen triple helix derives from the study of collagen-mimetic peptides (CMPs), which are short synthetic peptides (~30 residues) that feature the Xaa-Yaa-Gly repeats of collagen.^{3,4} In particular, the design of self-assembling CMPs, especially those that associate through “sticky ends” to form extended triple helices, enables CMPs to recapitulate the properties of biomaterials (Figure 1B).⁵ For example, sticky-ended CMP association underlies synthetic triple helices that match the length of their natural counterparts, hydrogels that replicate the rheology of natural collagens, and assemblies that promote cell adhesion.⁶

Sticky-ended self-assembly requires CMPs to associate with a large offset, forming single- and double-stranded extensions at each terminus of the growing triple helix (Figure 1C). Growth requires that sticky ends form triple helices with incoming peptide monomers or multimers that display complementary sticky ends. Thus, the interaction of the “double-stranded” collagen segments templated by the existing triple helix with unstructured single-stranded sections is critical for self-assembly. Additionally, recent work on animal models has revealed that short CMPs localize within wound beds when applied post-injury, which

suggests the presence of double-stranded collagens in physiological contexts.^{2,7} The structure of “double-stranded collagens,” however, remain unknown.

Here, we present the first examination of a double-stranded collagen model system. We investigate the stability, association, and structure of disulfide-linked pairs of (PPG)₁₀ strands (Figure 1E). Disulfide-templated strand dimers form stable triple helices when a third (PPG)₁₀ strand is present.⁸ Our data point to an intimate relationship between the strands of covalently linked CMP dimers, even in the *absence* of a third strand. The stability of double-stranded collagens necessitates a change in our conceptualization and elicitation of CMP self-assembly.

Previously, we showed that (PPG)₁₀ dimers covalently linked through various disulfide bridges support triple-helix formation.⁸ “Linked-dimers” can be generated by forming a disulfide bridge between leading (*s1x*) and lagging (*s3y*) strands, each having either a cysteine (Cys) or a homocysteine (Hcy) residue (Figures 2A and 2B). This way, four distinct “*x-y*” linked-dimers are formed, where “*x*” and “*y*” are either “*c*” or “*h*” for Cys or Hcy, identifying each linked-dimer by the residues that bridge its strands (Figure 2C). Mixing equimolar amounts of *x-y* with free (PPG)₁₀ (*s2*) produces a triple helix (*x-y·s2*). Irrespective of the chosen disulfide linker, *x-y·s2* complexes consistently exhibit a higher triple-helical content than does [(PPG)₁₀]₃, despite their lower thermostability.⁸ Further, the *x-y·s2* constructs appear as three-stranded units in solution, whereas free (PPG)₁₀ strands form monomer–trimer mixtures at equilibrium at 4 °C. We reasoned that the covalent linkage in *x-y* might aid triple-association by preorganizing the linked strands into a PPII-like structure in the absence of a third strand.

To determine if a linked-dimer can attain PPII-structure in the absence of a third strand, we examined the cystine-linked dimer, *c-c*, in the absence of a free *s2* strand. Remarkably, the *c-c* linked-dimer shares the characteristic circular dichroism (CD) signature of a collagen triple helix with *s2* (Figure 3A). Indeed, the linked-dimer exhibits slightly higher mean ellipticity at ~225 nm than does either *c-c·s2* or the *s2* triple helix, indicating more extensive PPII structure. Although the absence of the *s2* strand lowers the thermostability of “folded” *c-c* slightly (from a *T_m* of 28 °C to 24 °C), all three species exhibit similarly cooperative denaturation curves (Figure 3B).

These observations remain true for the *h-c* linked-dimer. The disulfide bridge installed in this construct can stabilize a triple-helical structure better than can a cystine linkage, and its use enhances the “triple-helical” structure of both the *h-c* and *h-c·s2* (Figure 3C). Interestingly, this improvement is more pronounced for the linked-dimer (*h-c*) than it is for the triple-helix (*h-c·s2*). Overall, CD data suggest well-structured linked-dimers with secondary structure reminiscent of a triple helix.

A single-residue stagger is necessary between collagen strands to associate into triple helices (Figure 1A), and disulfide bridges on *x-y* constructs were specifically designed to enable such association (Figure 2A).⁸ To probe the role of interstrand association on linked-dimer structure, we constructed the linked-homodimer, (*s1c*)₂. Although (*s1c*)₂ is an isomer of *c-c*, the strands of (*s1c*)₂ are not staggered and cannot associate (Figure 2D). Thus, in sharp

contrast to $c-c$, $(sIc)_2$ exhibits a weak collagen signal and an indistinct thermal transition even in the presence of $s2$ (Figure 3D). This same trend is observed when a pair of sarcosine residues, which disrupt triple-helical structure,⁹ are introduced into the sIh strand of $h-c$ (Figure S3). The strong dependence of PPII structure on the proper (*i.e.*, staggered and helical) association of linked strands suggests a collagen-like structure for linked-dimers.

Previously, we used analytical ultracentrifugation to show that equimolar mixtures of $x-y$ and $s2$ exist as three-stranded units in solution, a well-anticipated result verifying the formation of $x-y.s2$ triple helices.⁸ The preferred association state of a linked-dimer is, however, difficult to conceptualize, as the removal of the third strand renders numerous unpaired molecular contacts available for further association. Indeed, sedimentation equilibrium experiments reveal that $x-y$ linked-dimers are not free in solution, but rather dimerize into four-stranded units (Figure S4). In contrast, $(sIc)_2$ exists mostly as a monomer.

Trimerization of $x-y$, association of three linked-dimers into two triple helices, would have allowed a simple explanation for a strong $x-y$ CD signal. An $x-y$ dimer with four strands, however, can only produce a triple helix by leaving-out one strand. Such “triple-helical association” would diminish the CD signal with respect to $x-y.s2$, contrary to our data (Figures 3A–3C). Yet, dimerization of two linked-dimers without losing their double-helical character readily explains these observations (Figure S5). This interpretation is corroborated by the parallel impact of linker choice on the thermostability of all $x-y/x-y.s2$ pairs. The T_m value and the maximum CD signal for $x-y$ follows the patterns established previously for $x-y.s2$ triple helices (Figure 4). This correlation suggests an identical role for disulfide bridges in the context of a linked-dimer and of a triple helix. Computational models of $x-y$ and $x-y.s2$ further echo these parallels (Figure S6). Such consistency is unlikely with triple-helical association in which linkers take on multiple roles. For example, cystine-linked strands support a PPII fold when folding together (*e.g.*, $c-c$), but not when strand-donation is imperative (*e.g.*, $(sIc)_2$). Altogether, our results are consistent with double-helical association, which limits the role of disulfide bridges only to enhancing collagen-like association of intertwined strands (Figure S5).

To investigate further the nature of the dimerization of linked-dimers, we turned to nuclear magnetic resonance (NMR) spectroscopy. Installation of ^{15}N -glycine at specific sites on a CMP enables the study of local conformation and triple-helix formation. Amide chemical shifts in triple-helical and unfolded states have been determined for isotopically-labeled CMPs, especially $(\text{POG})_n$ variants.¹⁰ For analogous characterization, we synthesized $s2^n$, an ^{15}N -labeled $(\text{PPG})_{10}$ peptide. (Figure 5A). The $^1\text{H}, ^{15}\text{N}$ -HSQC spectra of $s2^n$ at 5 °C reveals two distinct peaks corresponding to folded $(\text{PPG})_{10}$ triple helices (upfield) and unfolded $(\text{PPG})_{10}$ strands (downfield), in line with earlier studies.¹⁰ Local symmetry leads to overlap of the signal from all strands of the triple helix, yielding a single “folded” peak.^{10c} This peak disappears when the temperature is raised above 37 °C, consistent with CD denaturation experiments (Figure 3B).

To monitor triple-helix formation by a linked-dimer, we placed ^{15}N labels on both strands of $h-c$, to obtain h^n-c^n (Figure 4B). The labels are equidistant from the N-terminus and the disulfide bridge, and are likely to experience similar chemical environments as neighbors in

the folded structure. As expected, the ^1H , ^{15}N -HSQC spectrum of $h^n\text{-c}^n\text{-s}2$ is nearly identical to that of $s2^n$ (Figure 4B), pointing to similar chemical environments in both triple helices. The effects of increasing temperature are likewise consistent—the $h^n\text{-c}^n\text{-s}2$ peak diminishes above the T_m (35 °C) in line with CD data (Figure 3C).

In the absence of a third strand, the $h^n\text{-c}^n$ linked-dimer produces a starkly different NMR spectrum (Figure 4C). Although the signal for unfolded strands remains, the peak associated with triple-helix formation is nearly absent and no new peaks are apparent. Thus, whereas a strong collagen signature on CD correlates well with a “folded” NMR signal for the triple-helical constructs ($h\text{-c-s}2$ and $s2$), triple-helix formation cannot explain the stronger CD signal observed for $h\text{-c}$. Instead, the data are consistent with the double-helical association model.

The association of a preorganized $x\text{-y}$ linked-dimer with $s2$ has kinetic and thermodynamic advantages over the formation of $s2$ triple helices. Previously, we demonstrated how interconnecting (PPG) $_{10}$ strands into linked-dimers enhances triple-helix formation.⁸ Our new data point to preorganization in linked-dimers even before they form triple helices. This preorganization is dependent on whether or not the disulfide bridge on the linked-dimer can template a triple helix. Constructs with non-templating linkers are not well-structured irrespective of the presence of a third strand (*cf.* Figures 3B and 3D). Similarly, linkers that better support collagen structure perform better as templates on linked-dimers (Figure 4). Thus, the structure of “double-helical” collagen relies on a sufficient triple-helix template.

Our results explain the success of self-assembling systems that rely on the sticky-ended association of CMPs.^{6a,6b,11,6c} Assembly initiation requires strands to associate with a large offset, producing a hypothetical homotrimer, only a small segment of which is triple helical (Figures 1B and 1C). The stability of templated strand pairs explains the viability of this otherwise-implausible species. Furthermore, such assemblies display templated strand pairs at each terminus of a growing triple helix. These “double-helical” sticky-ends are likely structured and well-poised to accept single strands. Likewise, CMP self-assemblies that place axial lysine–aspartic acid salt bridges on “double-helical” overhangs display higher thermostability and better fibers than do alternative designs.^{6c} These salt bridges could endow double-helical overhangs with stability that was not appreciated previously.¹¹

We conclude that the collagen “double helix” is a stable structural intermediate. Templated pairs of CMP strands interact tightly, exhibit a collagen-like fold, enable sticky-ended CMP association, and thereby, their self-assembly. Templated double helices are expected at sites of connective-tissue damage *in vivo*, and their stability elucidates the success of CMP-based tissue-damage detection methods and topical restorative treatments. We believe this discovery will illuminate aspects of collagen structure not appreciated previously, and provide new avenues for collagen-based nanotechnology.

Supplementary Material

Refer to Web version on PubMed Central for supplementary material.

ACKNOWLEDGMENT

We thank L. Nelavelli and Drs. M. D. Boersma, S. Chattopadhyay, and D. R. McCaslin for assistance with peptide synthesis and characterization; Dr. W. Chyan, J. M. Dones, H. R. Kilgore and Prof. M. T. Record, Jr. for helpful discussions; and Prof. S. H. Gellman for the use of his CD spectrometer.

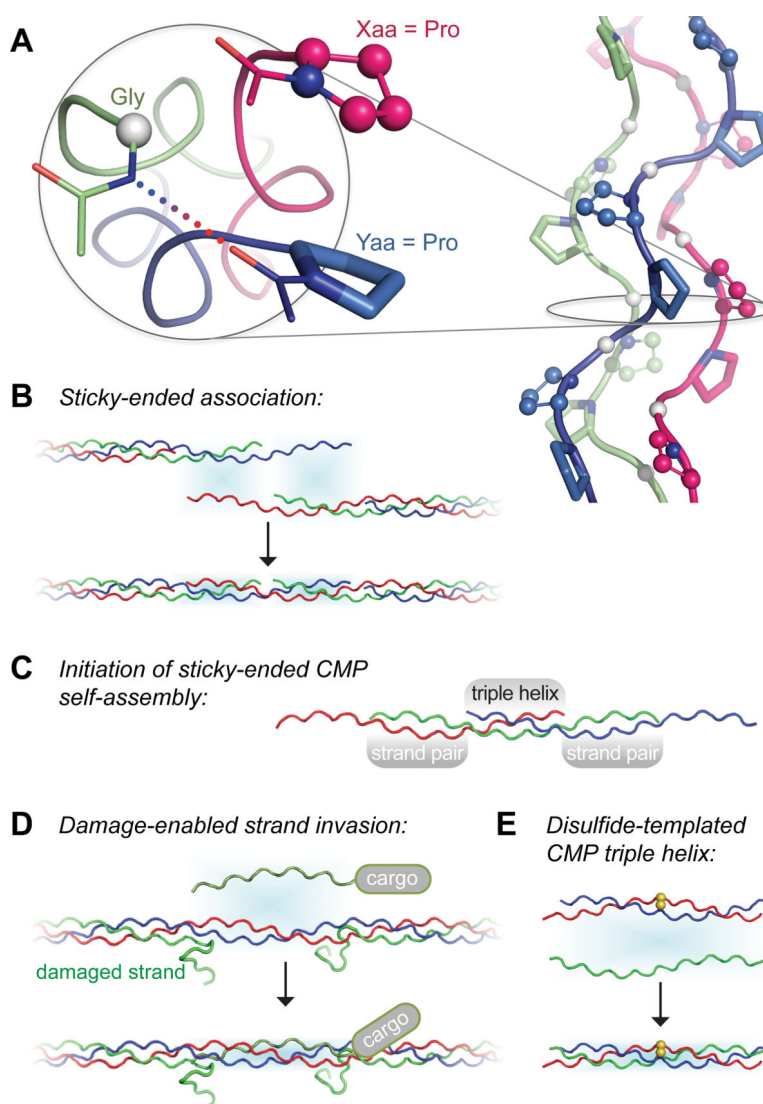
Funding

This work was supported by Grant R56 AR044276 (NIH). The Materials and Process Simulation Center was established with grants from DURIP-ONR, DURIP-ARO, and NSF-CSEM. NMRFAM was supported by Grant P41 GM103399 (NIH).

REFERENCES

- (1). Brinckmann J Collagens at a glance. *Top. Curr. Chem* 2005, 247, 1–6.
- (2). For reviews, see:(a)Meyers MA; Chen P-Y; Lin AY-M; Seki Y Biological materials: Structure and mechanical properties. *Prog. Mater. Sci* 2008, 53, 1–206.(b)Woolfson DN Building fibrous biomaterials from α -helical and collagen-like coiled-coil peptides. *Biopolymers* 2010, 94, 118–127. [PubMed: 20091877] (c)Fallas JA; O’Leary LER; Hartgerink JD Synthetic collagen mimics: Self-assembly of homotrimers, heterotrimers and higher order structures. *Chem. Soc. Rev* 2010, 39, 3510–3527. [PubMed: 20676409] (d)Przybyla DE; Chmielewski J Higher-order assembly of collagen peptides into nano- and microscale materials. *Biochemistry* 2010, 49, 4411–4419. [PubMed: 20415447] (e)Siebler C; Erdmann RS; Wennemers H From azidoproline to functionalizable collagen. *Chimia* 2013, 67, 891–895. [PubMed: 24594333] (f)Li Y; Yu SM Targeting and mimicking collagens via triple helical peptide assembly. *Curr. Opin. Chem. Biol* 2013, 17, 968–975. [PubMed: 24210894] (g)Chattopadhyay S; Raines RT Collagen-based biomaterials for wound healing. *Biopolymers* 2014, 101, 821–833. [PubMed: 24633807]
- (3). Shoulders MD; Raines RT Collagen structure and stability. *Annu. Rev. Biochem* 2009, 78, 929–958. [PubMed: 19344236]
- (4). Engel J; Bächinger HP Structure, stability and folding of the collagen triple helix. *Top. Curr. Chem* 2005, 247, 7–33.
- (5). Strauss K; Chmielewski J Advances in the design and higher-order assembly of collagen mimetic peptides for regenerative medicine. *Curr. Opin. Biotechnol* 2017, 46, 34–41. [PubMed: 28126669]
- (6). (a)Yamazaki CM; Kadoya Y; Hozumi K; Okano-Kosugi H; Asada S; Kitagawa K; Nomizu M; Koide T A collagen-mimetic triple helical supramolecule that evokes integrin-dependent cell responses. *Biomaterials* 2010, 31, 1925–1934. [PubMed: 19853297] (b)O’Leary LER; Fallas JA; Bakota EL; Kang MK; Hartgerink JD Multi-hierarchical self-assembly of a collagen mimetic peptide from triple helix to nanofibre and hydrogel. *Nat. Chem.* 2011, 3, 821–828. [PubMed: 21941256] (c)Tanrikulu IC; Forticaux A; Jin S; Raines RT Peptide tessellation yields micrometre-scale collagen triple helices. *Nat. Chem* 2016, 8, 1008–1014. [PubMed: 27768103]
- (7). (a)Chattopadhyay S; Murphy CJ; McAnulty JF; Raines RT Peptides that anneal to natural collagen in vitro and ex vivo. *Org. Biomol. Chem* 2012, 10, 5892–5897. [PubMed: 22522497] (b)Chattopadhyay S; Guthrie KM; Teixeira L; Murphy CJ; Dubielzig RR; McAnulty JF; Raines RT Anchoring a cytoactive factor in a wound bed promotes healing. *J. Tissue Eng. Regen. Med* 2016, 10, 1012–1020. [PubMed: 24677775] (c)Ellison AJ A pendant peptide endows a sunscreen with water-resistance. *Org. Biomol. Chem* 2018, 16, 7139–7142. [PubMed: 30256375] (d)Dones JM; Tanrikulu IC; Chacko JV; Schroeder AB; Hoang TT; Gibson ALF; Eliceiri KW; Raines RT Optimization of interstrand interactions enables burn detection with a collagen-mimetic peptide. *Org. Biomol. Chem* 2019, 17, 9906–9912. [PubMed: 31720665]
- (8). Tanrikulu IC; Raines RT Optimal interstrand bridges for collagen-like biomaterials. *J. Am. Chem. Soc.* 2014, 136, 13490–13493. [PubMed: 25211141]
- (9). Chen Y-S; Chen C-C; Horng J-C Thermodynamic and kinetic consequences of substituting glycine at different positions in a Pro-Hyp-Gly repeat collagen model peptide. *Biopolymers* 2011, 96, 60–68. [PubMed: 20560144]

- (10). (a) Li MH; Fan P; Brodsky B; Baum J 2-Dimensional NMR assignments and conformation of (Pro-Hyp-Gly)₁₀ and a designed collagen triple-helical peptide. *Biochemistry* 1993, 32, 7377–7387. [PubMed: 8338835] (b) Melacini G; Bonvin AMJJ; Goodman M; Boelens R; Kaptein R Hydration dynamics of the collagen triple helix by NMR. *J. Mol. Biol* 2000, 300, 1041–1048. [PubMed: 10903852] (c) Acevedo-Jake AM; Jalan AA; Hartgerink JD Comparative NMR analysis of collagen triple helix organization from N- to C-termini. *Biomacromolecules* 2015, 16, 145–155. [PubMed: 25579191]
- (11). Sarkar B; O’Leary LER; Hartgerink JD Self-assembly of fiber-forming collagen mimetic peptides controlled by triple-helical nucleation. *J. Am. Chem. Soc* 2014, 136, 14417–14424. [PubMed: 25494829]

**Figure 1.**

(A) Structure of the (PPG)₁₀ triple helix (right) and a cross-section highlighting the Xaa (balls & sticks), Yaa (sticks) and Gly positions (white balls). An interstrand hydrogen bond (dots) is shown between the preceding amide groups (sticks). (B–E) Templated collagen double helices recognize single-stranded CMPs. Yellow balls indicate a disulfide bond. See Supporting Information for a description of model building.

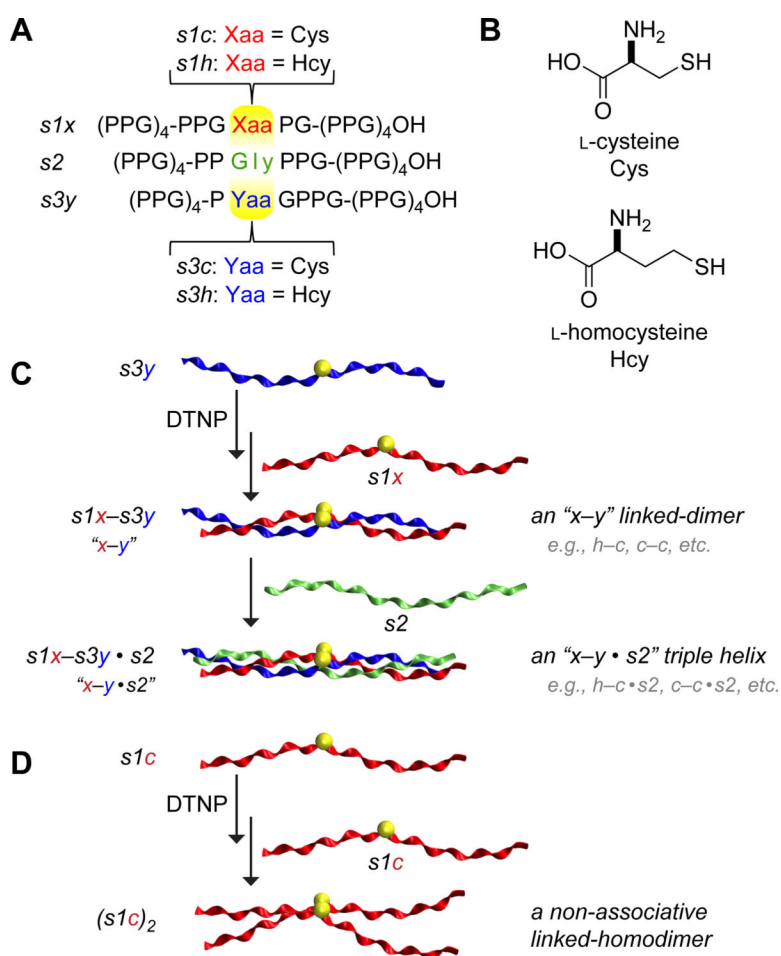
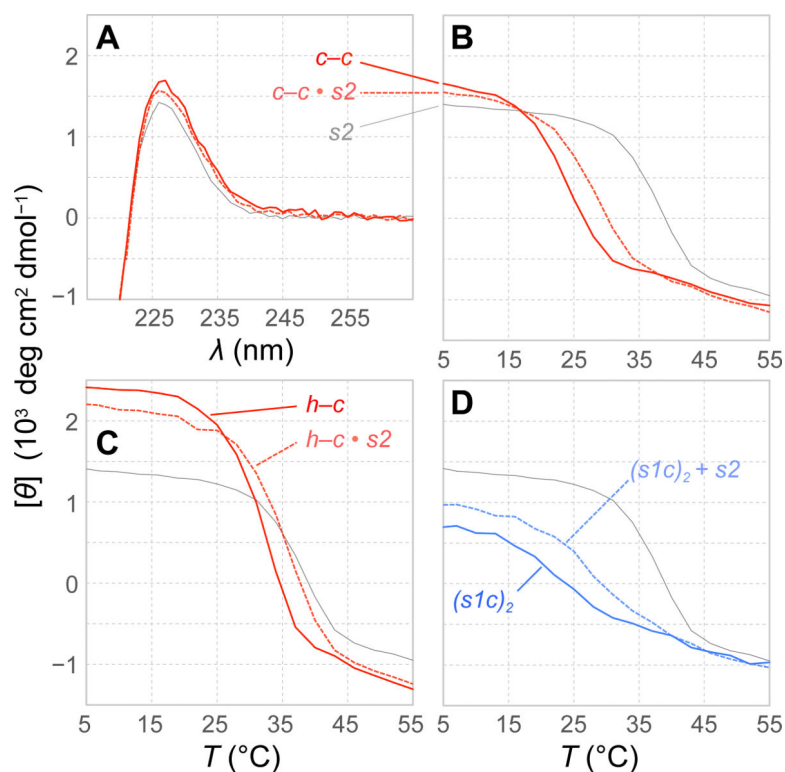


Figure 2. Design (A) and construction (C, D) of linked-dimers and triple helices through an Xaa–Yaa disulfide bridge. (B) Thioamino acids used. DTNP, 2,2'-dithiobis(5-nitropyridine).

**Figure 3.**

CD spectra (A) and thermal denaturation data (B) for $c-c$ linked-dimer and $c-c \cdot s2$ triple helix, thermal denaturation data for $h-c$ and $h-c \cdot s2$ (C) and $(s1c)_2$ linked-homodimer with and without $s2$ (D). For reference, $s2$ data (gray lines) is shown in all panels. Complete CD data can be found in Figures S2 and S3.

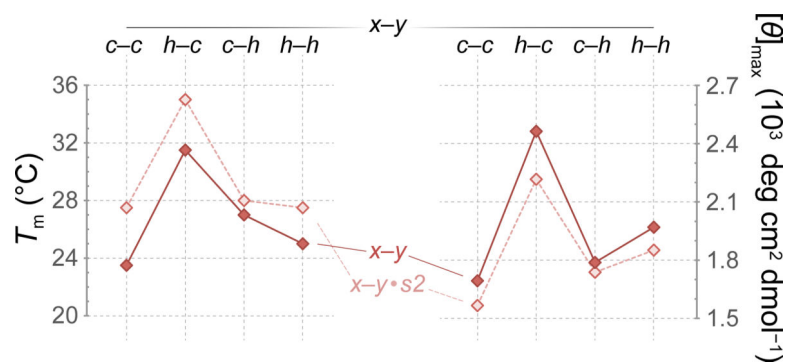
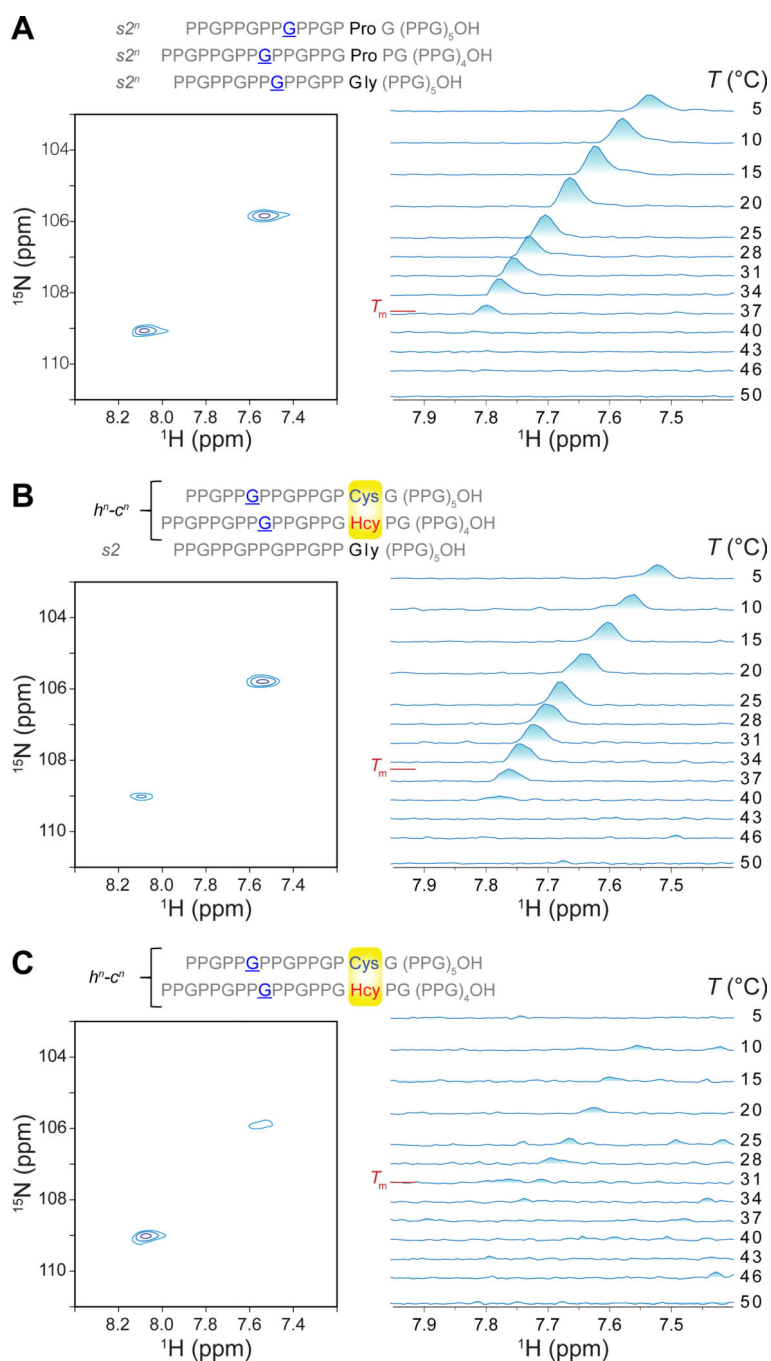


Figure 4. Comparison of T_m values and $[\theta]_{\max}$ at 4 °C for all $x-y$ (solid lines) and $x-y.s2$ (dashed lines). All CD data can be found in Figure S2.

**Figure 5.**

^1H , ^{15}N -HSQC NMR studies of triple-helix formation for the $s2^n$ (A) and $h^n-c^n \cdot s2$ triple helices (B), as well as the h^n-c^n linked-dimer (C). Residues with ^{15}N -labels are underlined, and a ^1H , ^{15}N -HSQC spectrum (at 5 °C) with a temperature-denaturation series is shown for each construct. Denaturation series tracks the triple-helix peak with increasing temperature. T_m of the construct determined by CD is indicated in red.